

# Plasma surface modification of epoxy polymer in air DBD and Gliding Arc

P Dimitrakellis<sup>1,2</sup>, F Faubert<sup>1</sup>, M Wartel<sup>1</sup>, E Gogolides<sup>2</sup> and S Pellerin<sup>1</sup>

<sup>1</sup>GREMI, Orleans University/CNRS, UMR 7344, F-18020 Bourges Cedex, France

<sup>2</sup>Institute of Nanoscience and Nanotechnology, NCSR “Demokritos”, Aghia Paraskevi 15341, Attiki, Greece  
E-mails: p.dimitrakellis@inn.demokritos.gr, stephane.pellerin@univ-orleans.fr

## Experimental details

### *Optical Emission Spectroscopy (OES)*

**Figure S1** presents the experimental set-up for the optical emission measurements, shown in this case for the Gliding Arc. Each discharge radiation was imaged by a set of two UV silica plano-convex lenses of 2'' diameter and 200 mm focal length into the entrance of a 10  $\mu\text{m}$  core diameter and 10 m length quartz optical fiber with a magnification factor 1. UV-visible radiations coming from the plasmas at the outlet of the optical fiber were collected into a Czerny Turner Spectrometer (ACTON SP2750i) equipped with two different gratings. The optical multichannel analyzer (OMA) placed at the outlet of the spectrometer was a 512 $\times$ 512 pixels iCCD camera (Princeton instrument PIMAX Gen2) used as light detector, cooled by Peltier effect module. All experimental parameters (dark current, linearity and stability of the photodetector) were measured or controlled. The spectral lines broadening due to the apparatus function, the effective linear dispersion and the wavelength calibration of the acquisition system have been determined using several narrow atomic emission spectral lines emitted by rare gas (Hg, Ne, and Ar) low pressure spectral lamps. The spectral response calibration of the acquisition chain over the 220 - 800 nm spectral range was performed using a calibrated deuterium-halogen lamp. Due to the weak signal of the calibration lamp collected between 200 and 220 nm leading to possible error in the calibration, the emission spectra from the plasmas below 220 nm were not considered in this study.

The adjustment of the camera parameter is controlled by a Pulsed Time Integrator (PTG) allowing a control of the temporal resolution of the recorded spectra (time integration, number of spectra, etc). Due to the relatively weak radiative emissions of the studied plasmas, the emission spectra were recorded by accumulation of 500 acquisitions having a gate width of 200 ms each for the DBD reactor experiments. Consequently, the spectrum represents an averaged in time and space plasma emission over several filaments. In case of Gliding Arc emission measurements, each spectrum corresponds to an accumulation of 100 acquisitions with a gate width of 200 ms to collect plasma emission over 1000 Gliding Arc discharges considering the mean lifetime of each of them.

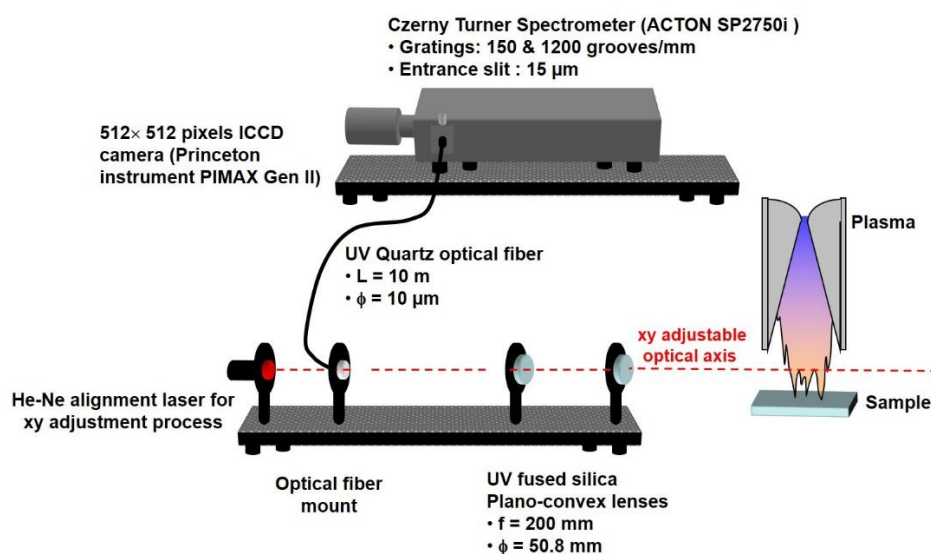


**Figure S1.** Overview of the optical setup for OES experiments: measurements for the Gliding Arc analysis.

### Temperature measurements

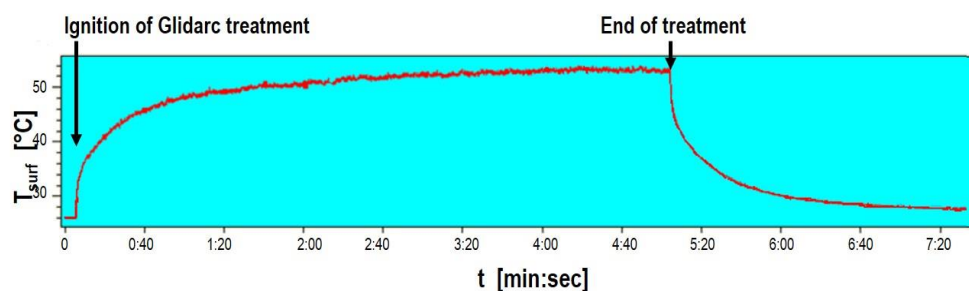


**Figure S2.** Evolution of the surface temperature of the epoxy sample under treatment with Gliding Arc as measured by infrared thermography.

## Results and discussion

### Optical Emission Spectroscopy (OES)

#### DBD

The vibrational ( $T_{\text{vib}}$ ) and rotational ( $T_{\text{rot}}$ ) temperatures of  $\text{N}_2(\text{C})$  have been determined by fitting each rovibrational structure of the  $\Delta v = 0, -1, -2$  and  $-3$  vibration bands. The uncertainties on the temperature values have been approximatively evaluated according to the sensible variation on the fitting results based on 5% accuracy on the peaks intensities. The vibrational temperature has not been calculated for the  $\Delta v = 0$  vibration band because only the band head is clearly observable on the spectrum. The calculation for the other observed vibration bands has not been considered for analysis due to the low signal to noise ratio.

Analysis of different vibrational bands of  $\text{N}_2$  show some discrepancies on the results according to vibration bands considered, as shown in **Table S1**. Indeed, the intensities ratio on the vibration peaks constituting a vibration band seems to reach any equilibrium according to a specific vibrational temperature, leading to results with significant uncertainties on the vibrational temperature. The rotational temperature determined with these

bands leads to nearby results as evaluated with the  $\Delta v = -1$  vibration band but the uncertainties on the values are higher probably due to the phenomenon mentioned above.

**Table S1.** Results for the vibrational ( $T_{\text{vib}}$ ) and rotational ( $T_{\text{rot}}$ ) temperatures determination for the ambient air DBD.

N <sub>2</sub> (2+) Vibration band	Spectral range (nm)	$T_{\text{vib}}$ (K)	$T_{\text{rot}}$ (K)
$\Delta v = 0$	329 - 341	Non evaluated	$605 \pm 100$
$\Delta v = -1$	349 - 361	$3045 \pm 100$	$605 \pm 50$
$\Delta v = -2$	370 - 382	$3436 \pm 400$	$582 \pm 100$
$\Delta v = -3$	393.5 - 406.5	$3027 \pm 300$	$576 \pm 100$

No specific errors on the calibration process have been detected during the analysis of the experimental data despite verification in this spectral range; then we can suppose that this phenomenon should be a result of the non-local thermal equilibrium character of this DBD discharge. The excitation equilibrium for rotation levels seems to be reached due to a fast thermal diffusion leading to a low value of the gas temperature (approximated to  $T_{\text{rot}}$ ). On the contrary, the population repartition over the vibrational levels is only partially equilibrated due to insufficient energy relaxation processes, observable by a higher temperature value. To conclude on this spectroscopy experiments on DBD reactor, the partial excitation equilibrium limited to the rotation levels allows to have a relatively accurate approximation of the rotational temperature, while the disequilibrium on the vibration state allows only questionable values of the vibrational temperature. Further investigations using a collisional-radiative model should be employed here to bring more precise and unambiguous results. Another hypothesis explaining these results is related to the experimental conditions. As the OES is a line-of-sight spectroscopic method, the obtained spectra correspond to an accumulation of the radiation of emitting species from the plasma all along the optical axis. Hence, strong variation of temperatures due to the filamentary character of the DBD generated plasma along this optical axis can cause some errors in the evaluation of the temperature based on the peaks intensity. This effect can explain the large difference between the rotational temperatures determined by emission spectroscopy, rather characteristic of the emissive zones of the discharge, and the average temperature of the plasma medium near the surface, estimated using the fiber optic temperature sensor (see **Table 1**).

#### Gliding Arc

**Table S2.** Results for the vibration ( $T_{\text{vib}}$ ) and rotation ( $T_{\text{rot}}$ ) temperatures determination for the Gliding Arc experiments.

Vibration band	Spectral range (nm)	$T_{\text{vib}}$ (K)	$T_{\text{rot}}$ (K)
OH A-X	305.5 – 309 (rough estimation)	Non evaluated	$3928 \pm 455$
OH A-X	305.5 - 318	$2767 \pm 200$	$4419 \pm 400$
OH A-X	305.5 - 310	$2609 \pm 200$	$3786 \pm 300$
N <sub>2</sub> C-B ( $\Delta v = -1$ )	349 - 361	$5493 \pm 2000$	$3508 \pm 800$

For the vibrational temperature, we observe a similar case as encountered with N<sub>2</sub> calculation on DBD plasma emission, the respect of the intensity ratio between the two vibration peaks detected remains difficult to fit with the software Specair® leading to higher value of the  $T_{\text{vib}} = 5493 \pm 2000$  K and a significant uncertainty because of these noisy unknown peaks. The vibrational temperatures deduced from the OH spectrum, that are considerably lower than those of N<sub>2</sub>, are probably questionable and will not be considered.

As has already been reported by various authors [1, 2], the vibrational temperatures calculated from OH emissions differ significantly from those of other species, especially in non-equilibrium flows. These different obtained values of  $T_{\text{vib}}$  depending on the molecules (OH or  $\text{N}_2$ ) can be explained by the non-LTE character of the Gliding Arc in these experimental conditions where the sample is very close to the electrodes, and it induces several disturbances on the air flow and the plasma plume. Unfortunately, the calculation on the  $\Delta v = -2$  vibration bands (not presented) do not bring some additional information to confirm the hypothesis; the very noisy spectrum due to the very weak  $\text{N}_2$  radiation do not permit to converge to realistic values both for vibration and rotation temperature. Zhu *et al* [3] use the NO A–X transition at a wavelength range of 211–239 nm to determine the vibrational temperature of the Gliding Arc discharge, based on the ratio of the two peak intensities of the NO A–X (1, 0) at about 214.7 nm and the NO A–X (0, 1) band at about 236 nm bands. Unfortunately, we could not apply this method to verify the  $T_{\text{vib}}$  measured by  $\text{N}_2$ , given the difficulty in extracting the continuous background in this spectral range on our recordings.

In the Gliding Arc spectroscopic analysis, the results obtained for the rotational temperature seem to be coherent and similar for all the tested molecules highlighting the quasi-complete equilibrium of the rotation states in this discharge. The results concerning the vibration temperature remains more questionable according to the relative low convergence between the experimental results and the fitting process, but the discrepancy between the experimentally measured OH(A) and  $\text{N}_2(\text{C})$  vibrational temperatures is indicative of the nonequilibrium flow field. We presume that in our Gliding Arc conditions, perturbation of the plasma plume by the sample can be a cause of non-equilibrium between the vibration states. As mentioned in DBD experiments, another possibility explaining the results remains the significant variation of the vibration temperature along the optical axis. In this case, the intensity ratio observed on the spectrum corresponds to an overlap of multiple different equilibria which cannot be fitted by a single vibration temperature. However, its value is very high compared to the average gas temperature in the vicinity of the surface of the sample, determined using the optical fiber (see Table 1): this is probably due to the fact that the measurements by emission spectroscopy are integrated both spatially (along the optical line of sight) and temporally (integrating several passes of plasma discharges in front of the detector), and are characteristic of the successive discharges periodically sweeping the surface.

## References

- [1] Sharma M, Austin J M and Glumac N G, 2010, NO and OH Spectroscopic Vibrational Temperature Measurements in a Postshock Relaxation Region, *AIAA Journal*, **48**-7, doi: 10.2514/1.J050047
- [2] Zhao T L, Xu Y, Song Y H, Li H S, Liu J L, Liu J B, and Zhu A M, 2013, Determination of vibrational and rotational temperatures in a gliding arc discharge by using overlapped molecular emission spectra, *J. Phys. D Appl. Phys.* **46**, 345201
- [3] Zhu J, Ehn A, Gao J, Kong C, Alden M, Salewski M, Leipold F, Kusano Y and Li Z, 2017, Translational, rotational, vibrational and electron temperatures of a gliding arc discharge, *Optics Express*, **25**-17, 20243, doi: 10.1364/OE.25.020243